Electronic Supplementary Material (ESI) for Nanoscale Advances.
This journal is © The Royal Society of Chemistry 2022

Electronic supporting information

Strain engineering of graphene on rigid substrates

Yang Zhang [a], Yanhan Jin [a], Jinglan Liu [a], Qiancheng Ren [a], Zhengyang Chen [b], Yi Zhao [b], Pei Zhao [a,c,]*

[a] Center for X-Mechanics and Institute of Applied Mechanics, Zhejiang University, Hangzhou 310027, P. R. China

[b] College of Information Science and Electronic Engineering, Zhejiang University, Hangzhou 310027, P. R. China

[c] State Key Laboratory of Fluid Power and Mechatronic Systems, Zhejiang University, Hangzhou, 310027, P. R. China

*Email: peizhao@zju.edu.cn

KEYWORDS: graphene, strain engineering, transfer, rigid substrates, capillary force

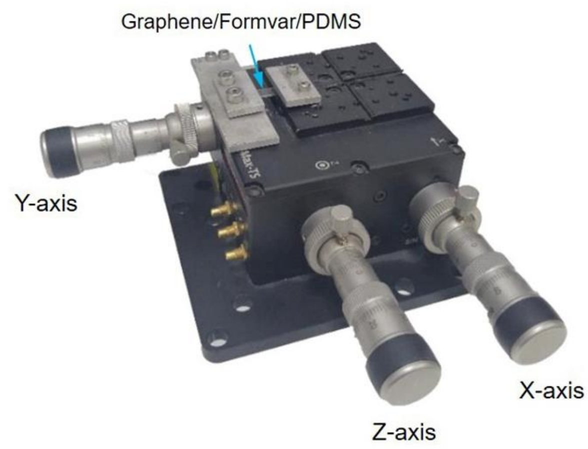

Fig.S1 Home-made tensile testing machine.

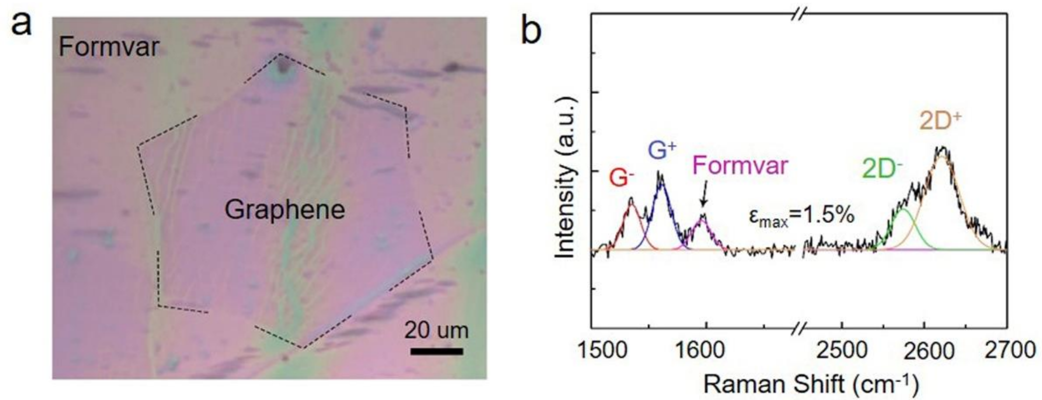

Fig.S2 Sandwich structure of Formvar/Graphene/SiO_2. (a) OM image of formvar/graphene/SiO_2. (b) Raman spectrum of strained graphene under formvar.

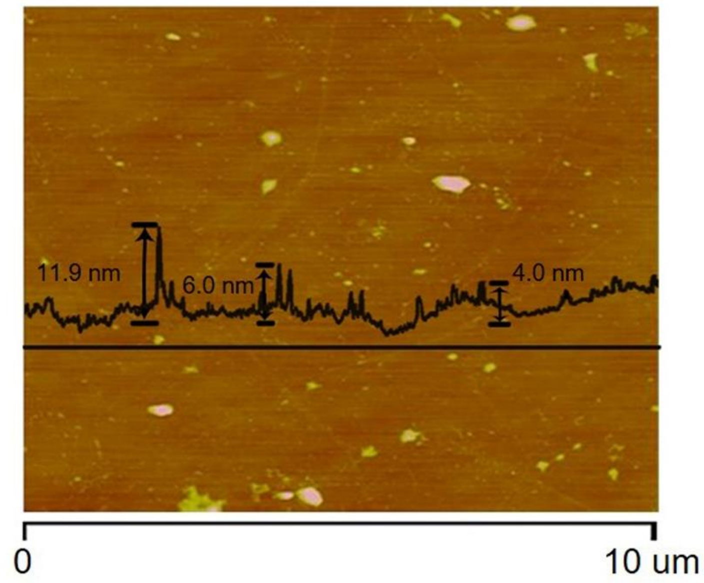

Fig.S3 AFM image of graphene transferred by PMMA.

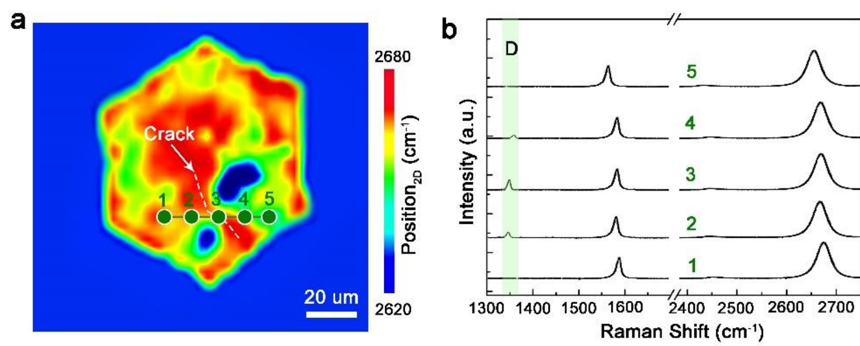

Fig.S4. Raman spectrum of strained graphene on SiO_2/Si substrate. (a) Raman map of the 2D peak positions of the strained graphene. (b) Representative Raman spectra of graphene in (a).

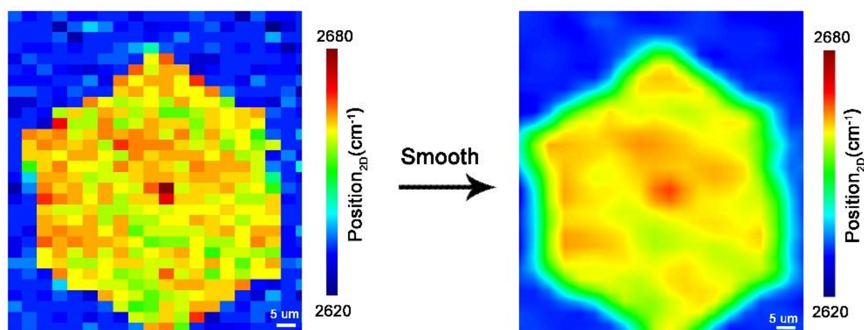

Fig. S5. The effect of smoothing for Raman maps.

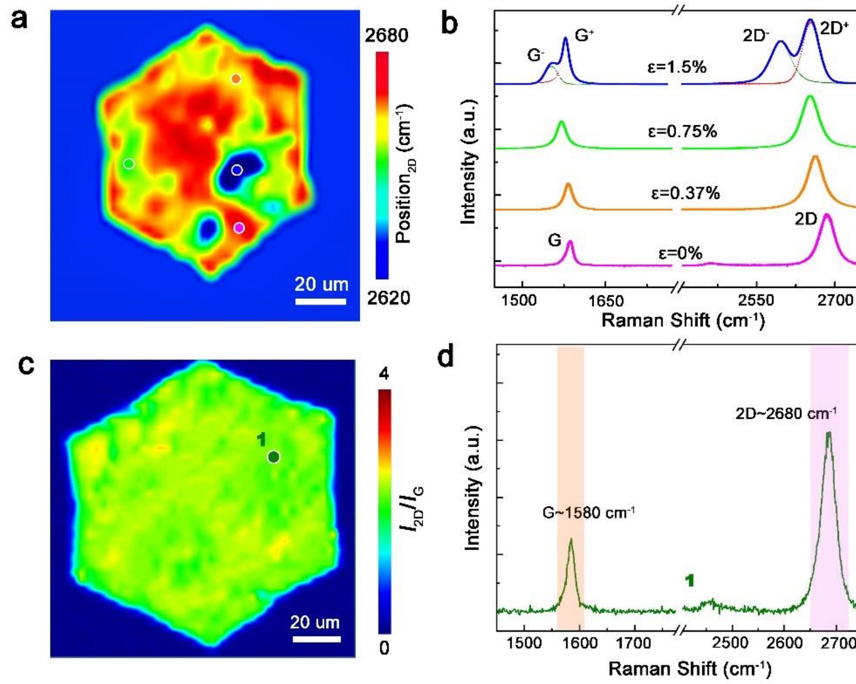

Fig.S6. Raman spectrum of unstrained graphene on SiO_2/Si substrate. (a) Raman map of the 2D peak positions of the strained graphene. (b) Representative Raman spectra of graphene in circled regions in (a). (c) Raman maps of I_{2D}/I_G of unstrained graphene. (d)Raman spectra of graphene marked in (c). ((a) and (c) are adopted from Figure 2(d) and (e) in manuscript, respectively)

The fitted peak parameters of the blue region in Figure R1(a) are G^-~1532 cm^{-1}, G^+~1564 cm^{-1}, $2D^-$~2597 cm^{-1}, and $2D^+$~ 2638 cm^{-1} as shown in Figure R1(b). The calculation process of the strain value is as follows:

Firstly, in order to exactly obtain the frequency of the Raman peak at zero strain, we transferred an unstrained graphene onto SiO_2/Si substrate by the same procedure except for stretching in Figure R1 (c). As shown in Figure R1 (d), the position of G peak at zero strain (ω_G^0) is 1580 cm^{-1}, and the position of 2D peak at zero strain (ω_{2D}^0) is 2680 cm^{-1}. Then inserting the coefficients of $\gamma = 1.99$ and $\beta = 0.99$ in Eq.S1,[A. Bosak, M. Krisch, M. Mohr, J. Maultzsch, and C. Thomsen, Phys. Rev. B 75, 153408 2007. ;A. Bosak, M. Krisch, M. Mohr, J. Maultzsch, and C. Thomsen, Phys. Rev. B 75, 153408 2007.]:

$$\triangle\omega_G^{\pm} = -\gamma\omega_G^0(\varepsilon_{ll} - \varepsilon_{tt}) \pm \frac{1}{2}\beta\omega_G^0(\varepsilon_{ll} - \varepsilon_{tt}) \quad \text{S1}$$

a uniaxial strain of 1.53% can be derived from the $G^{\pm}$ peak, which is consistent with the strain value of 1.5% mentioned in manuscript. Besides, the position of G peak in the yellow and green regions of Figure R1(b) are 1533 cm^{-1} and 1557 cm^{-1}, respectively. Using Eq.R1, the strain value of 0.75% and 0.37% can also been derived respectively. As for the strain value derived from 2D peak, we directly use the value of Raman peak shifts for and 2D peak components per percentage of strain (~-64 cm^{-1}/%) as mentioned in the same references of (T.M.G. Mohiuddin et al., Phys. Rev. B 79 (2009) 205433). The peak shifts of 2D in the yellow and green regions of Figure S6(b) are -48 and -24 cm^{-1}, corresponding to strain values of 0.75% and 0.37%, respectively.

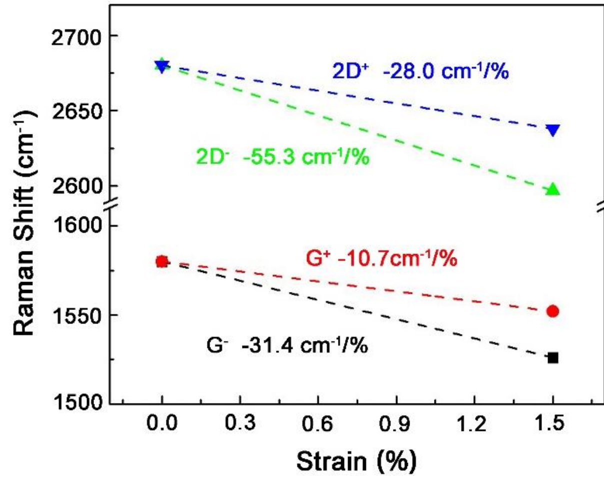

Figure S7. The peak shifts of the decomposed subpeaks for the Raman G and 2D peaks as a function of the strain value.

In order to confirm the strain value, we plotted the peak shifts of the decomposed subpeaks for the Raman G and 2D peaks as a function of the strain value as shown in Figure S7. The slopes of the fitted lines that represent the shifting rates of graphene's Raman peaks are $\partial\omega_{G^+} / \partial\varepsilon \sim -10.7$, $\partial\omega_{G^-} / \partial\varepsilon \sim -31.4$, $\partial\omega_{2D^+} / \partial\varepsilon \sim -28$, $\partial\omega_{2D^-} / \partial\varepsilon$ ~ –55.3 cm $^{-1}$/%, which is similar to the results obtained by other publications as shown in Table S1.

Table S1. Comparison of Raman peak shifts for G (2D) peak components per percentage of strain

Reference	$\partial\omega / \partial G$ (cm^{-1}/%)		$\partial\omega / \partial 2D$ (cm^{-1}/%)	
	$\partial\omega / \partial G^+$	$\partial\omega / \partial G^-$	$\partial\omega / \partial 2D^+$	$\partial\omega / \partial 2D^-$
This work	**-10.7**	**-31.4**	**-28.0**	**-55.3**
Ref. 1	-10.8	-31.7	----	----
Ref. 2	-16.6	-35.2	-28.0	-56.7
Ref. 3	-14.2	-31.8	-21.9	-55.5

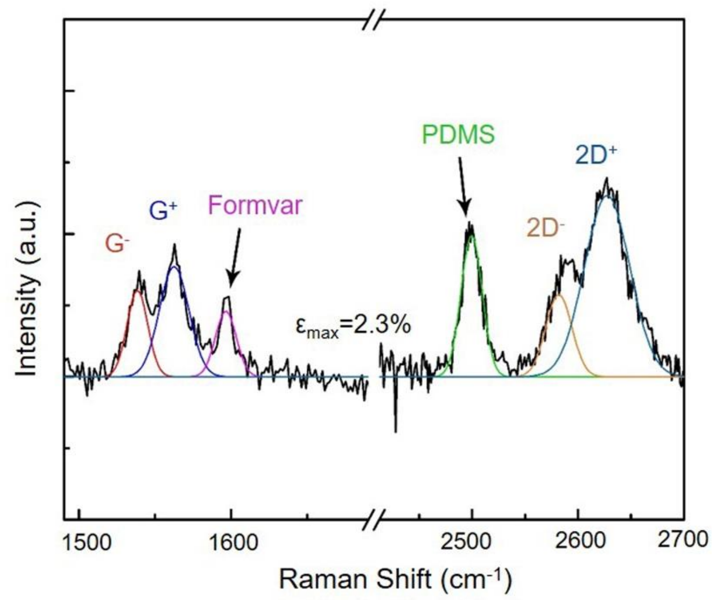

Fig.S8 Raman spectrum of strained graphene on PDMS.

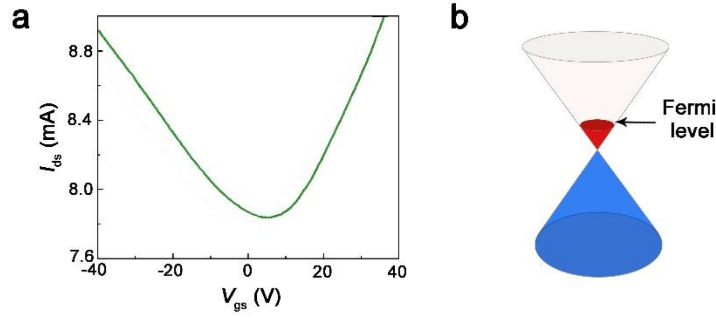

Fig. S9. Electric performances of unstrained graphene on SiO_2/Si substrate. (a) Transfer characteristic curves of devices fabricated by unstrained graphene. (b) Schematic illustration of the Fermi level derived from the unstrained graphene.

As shown in Fig. S9 (a), the V_{Dirac} is about 8.2 V, and its carrier concentration (*n*) of the neutral point can be derived from the following equation:[4]

$$V_{Dirac} = e\frac{n}{C_g} \qquad \text{S2}$$

C_g is the gate capacitance of SiO_2 substrate and e is the elementary charge. By inserting $V_{Dirac} = 8.2$ V and $C_g = 1.21\times10^{-8}$ F·cm^{-2} ,[5] we obtain the carrier content is about 4×10^{11} cm^{-2}, corresponding the Fermi level of about 4.68 meV, which indicates the graphene has slightly *p*-doped as schematically shown in Figure S9(b).[6] However, we think this doping may has little effect on the calculation of the strain value of graphene, since these two devices were fabricated by the same procedure.

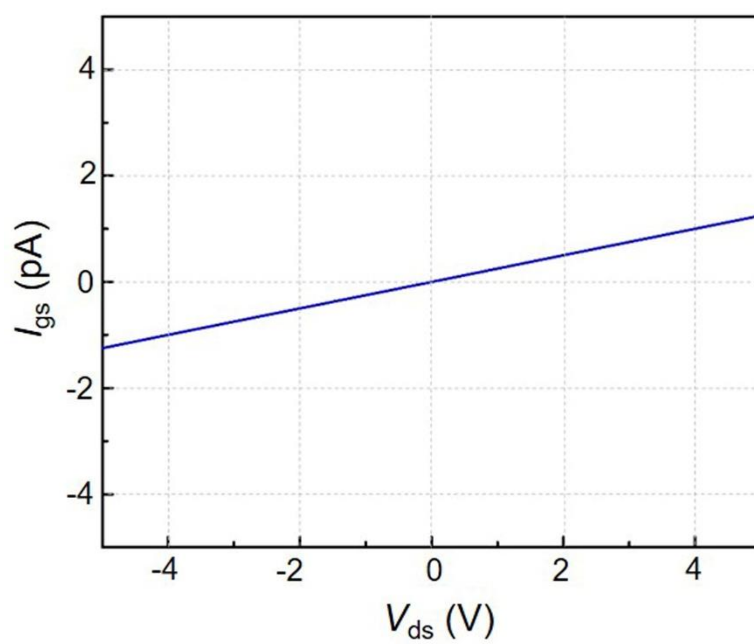

Fig.S10 Leakage current of fabricated graphene FET.

Reference:

1. T. M. G. Mohiuddin, A. Lombardo, R. R. Nair, A. Bonetti, G. Savini, R. Jalil, N. Bonini, D. M.

   Basko, C. Galiotis, N. Marzari, K. S. Novoselov, A. K. Geim and A. C. Ferrari, *Phys. Rev. B*, 2009, **79**.
2. Y. L. Wang, Y. Wang, C. Xu, X. W. Zhang, L. Mei, M. Wang, Y. Xia, P. Zhao and H. T. Wang, *Carbon*, 2018, **134**, 37-42.
3. Y. Jin, Q. Ren, J. Liu, Y. Zhang, H. Zheng and P. Zhao, *Exp. Mech.*, 2022, **62**, 761-767.
4. C. Jang, S. Adam, J. H. Chen, E. D. Williams, S. Das Sarma and M. S. Fuhrer, *Phys. Rev. Lett.*, 2008, **101**, 146805.
5. W. S. Leong, H. Z. Wang, J. J. Yeo, F. J. Martin-Martinez, A. Zubair, P. C. Shen, Y. W. Mao, T. Palacios, M. J. Buehler, J. Y. Hong and J. Kong, *Nat. Commun.*, 2019, **10**, 1-8.
6. P. H. Ho, Y. C. Yeh, D. Y. Wang, S. S. Li, H. A. Chen, Y. H. Chung, C. C. Lin, W. H. Wang and C. W. Chen, *ACS Nano*, 2012, **6**, 6215-6221.